current issues in molecular biology

MDPI

Article

Periplasmic Expression and Characterization of an Alpha-Synuclein Preformed Fibril-Specific Nanobody and Its Antigen in *Escherichia coli* W3110 and W3110 Δ*OMPC*

Huy Nguyen-Thanh, Anh Nguyen-Tu and Thai Nguyen-Minh *

School of Pharmacy, University of Medicine and Pharmacy, Ho Chi Minh City 700000, Vietnam
* Correspondence: minhthai2511@ump.edu.vn

Abstract

The abnormal accumulation of alpha-synuclein (α-syn) is a core pathogenic mechanism in Parkinson's disease. The nanobody PFFNB2 inhibits α-syn pre-formed fibrils (α-syn PFF) but faces expression challenges due to the absence of a canonical disulfide bond. This study aimed to express PFFNB2 and α-syn in the periplasm of *Escherichia coli* (*E. coli*) W3110 and its ompC-deficient mutant (Δ*ompC*). PFFNB2 was expressed with and without a Maltose Binding Protein (MBP) fusion tag, while α-syn was expressed tag-free. Periplasmic proteins were extracted via osmotic shock, purified using chromatography, and analyzed for molecular weight and expression yield. The amyloid fibril-forming capacity of α-syn was evaluated using a Thioflavin T assay, and apparent binding potency was assessed via ELISA. Results demonstrated successful cloning, expression, and purification of both proteins. MBP-PFFNB2 yielded higher expression yield than the MBP-free form. Although the Δ*ompC* mutant showed a lower nanobody expression yield than the wild-type strain, the MBP-PFFNB2 obtained from this mutant exhibited optimal activity and specifically bound to α-syn PFF (EC_{50} of 0.3445 nM). Regarding α-syn, the Δ*ompC* mutant provided a superior expression yield, and lactose induction significantly reduced the formation of toxic oligomeric forms. In conclusion, combining periplasmic expression, an MBP fusion tag, and the *E. coli* W3110 Δ*ompC* strain creates a potential system for producing PFFNB2 nanobodies with high anti-α-syn PFF activity.

Keywords: alpha-synuclein; *E. coli* W3110; *E. coli* W3110 Δ*ompC*; nanobody; PFFNB2

1. Introduction

Parkinson's Disease (PD) is the second most common neurodegenerative disorder globally and is increasing at an alarming rate, causing motor and non-motor symptoms that severely affect patients' quality of life [1]. Central to the pathogenesis of PD is the abnormal accumulation of alpha-synuclein (α-syn) [2]. In pathological environments, α-syn misfolds and aggregates into toxic forms such as oligomers and fibrils, ultimately forming Lewy bodies within cells. These protein aggregates are highly toxic, as they attack cell membranes, impair mitochondrial function, increase oxidative stress, and disrupt the cellular protein clearance system. Furthermore, pathological α-syn can spread from cell to cell via a prion-like mechanism, allowing the defective proteins to migrate from diseased to healthy cells, converting normal proteins into pathological forms, and disseminating damage throughout the nervous system [3]. Therefore, the search for disease-modifying therapies that directly intervene in the α-syn-centric pathogenesis is currently a major focus in modern medicine.

Check for updates

Academic Editor: Fabrizio De Luca

Received: 7 October 2026
Revised: 19 October 2026
Accepted: 21 October 2026
Published: 23 October 2026

Copyright: © 2026 by the authors. Licensee MDPI, Basel, Switzerland. This article is an open access article distributed under the terms and conditions of the Creative Commons Attribution (CC BY) license.

Among strategies targeting α-syn, immunotherapy using traditional monoclonal antibodies faces significant barriers due to their bulky molecular size (approximately 150 kDa), resulting in an extremely low rate of antibodies crossing the blood–brain barrier. Consequently, they are unable to access epitopes buried within amyloid aggregates and carry the risk of triggering excessive neuroinflammatory responses via Fc receptors [4]. In contrast, single-domain antibodies (nanobodies), with their ultra-small size (only about 15 kDa), in theory can offer superior tissue penetration, easily navigating into the narrow crevices of the amyloid core structure. Over more than a decade of development, a series of α-syn-targeting nanobodies has been generated, ranging from recognizing basic monomers to precisely targeting specific toxic structures [4–7]. However, these nanobodies bind to total α-syn, encompassing both normal physiological monomers and disease-associated aggregates. Consequently, the highly abundant α-syn monomers in cells compete for nanobody binding, reducing the therapeutic efficacy against toxic aggregates while potentially disrupting the critical physiological functions of α-syn monomers at synapses.

To overcome this challenge, the nanobody PFFNB2 was engineered to bind tightly and preferentially to α-syn preformed fibrils (α-syn PFF) while exhibiting very weak affinity for the monomeric form [8]. Although PFFNB2 cannot prevent the initial aggregation of α-syn monomers, it is capable of disassembling fibrillar structures in vitro, inhibiting the prion-like pathological spread of α-syn from one brain region to another. However, α-syn PFFs are primarily localized intracellularly, whereas conventional nanobodies are studied under extracellular conditions or within the periplasmic space. As a result, intracellular antioxidants (present to protect cells from oxidative stress) reduce the disulfide bonds, destabilizing the nanobody structure and leading to a loss of activity. Consequently, PFFNB2 was designed to be completely devoid of disulfide (S-S) bonds right from the extracellular screening stage, ensuring the nanobody folds properly even when introduced intracellularly. This characteristic lack of S-S bonds, while necessary (since reintroducing the S-S bond into PFFNB2 diminishes its activity), presents expression challenges, making it imperative to express PFFNB2 as a fusion with Maltose Binding Protein (MBP) alongside the supplementation of the GroEL/GroES chaperone pair.

To address the aforementioned issue, the periplasmic expression system of *Escherichia coli* (*E. coli*) bacteria emerges as a potential alternative [9]. Unlike the strongly reducing environment of the cytoplasm, which often leads to protein aggregation and inclusion body formation, the periplasm provides an ideal oxidizing environment along with a natural chaperone network that directly assists in proper protein folding. Furthermore, because the periplasm occupies only about 20% of the cell volume and contains significantly fewer endogenous proteins than the cytoplasm, the target protein can be easily released using the osmotic shock technique, facilitating the removal of a large amount of impurities right from the initial step.

Regarding the choice of expression strain, the *E. coli* K-12 W3110 strain is considered an ideal host cell due to its high genetic stability and robust physiological characteristics [10]. *E. coli* W3110 has also established its critical role in the development of immunotherapies, having been used as a platform for producing recombinant Fab fragments. Moreover, its outer membrane porin-deficient mutant, *E. coli* W3110 Δ*ompC*, exhibits significant alterations in outer membrane permeability and metabolic networks, offering tremendous potential in supporting accurate protein folding, enhancing inducer uptake, and increasing sensitivity to detergents, thereby simplifying the lysis process for product recovery [11].

Based on these points, in this study, we conducted experiments to express, extract, and purify PFFNB2, MBP-PFFNB2, and tag-free alpha-synuclein from the periplasmic space of both the wild-type *E. coli* W3110 strain and the *E. coli* W3110 Δ*ompC* mutant. The molecular weight of the target proteins, the protein expression yield of the two *E. coli* strains, and

the specific binding affinities of the nanobodies to different forms of alpha-synuclein were evaluated, thereby providing novel insights into the expression characteristics of PFFNB2 as well as the feasibility of expressing this antibody–antigen pair in *E. coli* W3110 and its Δ*ompC* mutant.

2. Materials and Methods

2.1. Materials

The synthesized PFFNB2 gene product (Yemima Butler et al. [8]) and cloning primers were provided by Phu Sa Genomics JSC (Can Tho, Vietnam). The synthesized human α-syn gene product (UniProt #P37840) was provided by GenScript Biotech (Nanjing, China). Employed plasmids include: pBXNPH3 (Addgene plasmid #110098; https://n2t.net/addgene:110098 (accessed on 20 October 2026); RRID:Addgene_110098) and pBXNPHM3 (Addgene plasmid #110099; https://n2t.net/addgene:110099 (accessed on 20 October 2026); RRID:Addgene_110099), both were a gift from Markus Seeger [12] for PFFNB2 expression, and pTrcECT (Addgene plasmid #75477; https://n2t.net/addgene:75477 (accessed on 20 October 2026); RRID:Addgene_75477) was a gift from Xixian Xie [13] for α-syn expression. Plasmids were extracted using the DNA-spinTM plasmid DNA purification kit, cloning product purification was performed using the MEGAquick-spinTM plus total fragment DNA purification kit, and DNA ladders (SiZer™-1000/100 DNA Marker) were all provided by iNtRON Biotechnology (Seongnam-si, South Korea). The *E. coli* DH5α strain, restriction enzymes (*Bsp*QI, *Eco*RI, *Bam*HI), T4 DNA Ligase, and Prestained Protein Standard, Broad Range (10–250 kDa) were provided by New England Biolabs (Milton Park, UK). PCR reactions were performed using the AccuStart™ II PCR ToughMix® kit from Quantabio (Beverly, MA, USA). The expression strains, wild-type *Escherichia coli* W3110 (*E. coli* FΛrph1 IN(rrnDrrnE)1) and *Escherichia coli* W3110 Δ*ompC*, were part of our lab's strains collection. Proteins were purified using the ÄKTA start™ FPLC system from Cytiva (Marlborough, MA, USA). The α-syn aggregation reaction was carried out in Low Protein Binding Microcentrifuge Tubes from Thermo Scientific (Waltham, MA, USA). The ThT Assay was performed with Thioflavin T from Sigma (Waltham, MA, USA) and read on a Biotek Synergy HTX 96-well microplate reader from Agilent BioTek (Winooski, VT, USA). In the ELISA, Mouse 6x-His Tag Monoclonal Antibody (HIS.H8) and Horseradish Peroxidase (HRP)-conjugated Goat anti-Mouse IgG Antibody were provided by Invitrogen (Carlsbad, CA, USA). Sonication was performed using QSONICA Q700 Sonicator with microtip, manufactured by Qsonica (Newtown, CT, USA). Cloning simulations were performed using Snapgene 8.2.2 software provided by GSL Biotech, LLC (Boston, MA, USA); graphs and EC_{50} results were generated using Graphpad Prism 10 software, provided by GraphPad Software (San Diego, CA, USA).

2.2. Cloning and Expression of PFFNB2, MBP-PFFNB2, and Tag-Free α-syn

First, the genes encoding PFFNB2 and α-syn were PCR-amplified to create overhangs containing the respective restriction enzyme cleavage sites. Details of primer pairs used in this study are listed in Supplementary Materials (Table S1). Notably, the PFFNB2 gene was amplified to introduce flanking *Bsp*QI restriction sites along with a C-terminal Avitag sequence for potential downstream biotinylation applications. The resulting fragments were ligated into pBXNPH3 and pBXNPHM3 vectors to generate pelB-10xHis-PFFNB2-Avitag and pelB-10xHis-MBP-PFFNB2-Avitag constructs. Meanwhile, the α-syn-encoding gene was digested and ligated into pTrcECT via *Eco*RI and *Bam*HI restriction sites to generate tag-free α-syn. The recombinant vectors were then chemically transformed into the *E. coli* DH5α strain. Colony PCR was performed using the pBAD Forward and pBAD Reverse primer pair to select colonies carrying pBXNPH3/pBXNPHM3_PFFNB2. Similarly, the PtrcPro-F

and rrnB-T1-term-Rev primer pair was used to select colonies carrying pTrcECT_α-syn. The vectors were subsequently extracted and further chemically transformed into *E. coli* W3110 and *E. coli* W3110 Δ*ompC*.

The following day, 1 colony from each successfully transformed plate was inoculated into 5 mL of LB (Luria–Bertani) medium supplemented with 100 µg/mL Ampicillin and incubated overnight with shaking at 200 rpm at 37 °C. The next morning, 1 mL of the overnight bacterial culture was added to a 1-L shake flask containing 100 mL of TB medium (supplemented with 10X TB Buffer and 100 µg/mL Ampicillin). The bacteria were incubated with shaking at 200 rpm at 37 °C until the OD_{600} reached between 0.6 and 0.8, after which the temperature was reduced to 22 °C, and the bacteria were incubated for an additional hour. Finally, inducers including Arabinose (final concentration 0.02% (*w*/*v*)) for the pBX vectors and IPTG (final concentration 0.2 mM) or Lactose (final concentration 2% (*w*/*v*)) for the pTrc vector were added to the culture medium. The bacteria were induced with shaking at 200 rpm at 22 °C. The total induction time was 12 h for the pBX vectors and 10 h for the pTrc vector.

*2.3. Extraction of Nanobodies and α-syn from the Periplasmic Space of E. coli W3110 and E. coli W3110 Δ*ompC*

Nanobodies were extracted using the osmotic shock method supplemented with lysozyme, adopted from Zimmermann et al. [14]. First, the cell biomass after overnight induction was centrifuged at 5000× *g* for 15 min at 4 °C. The cell pellet was then resuspended in Periplasmic Extraction Buffer N (20% (*w*/*v*) Sucrose; 50 mM Tris-HCl (pH 7.4); 0.5 mM EDTA; 0.5 µg/mL Lysozyme) (4 mL of buffer per 40 mL of centrifuged bacterial culture). The suspension was incubated on ice for 30 min. The cells were then subjected to osmotic shock by rapidly adding cold 1X TBS up to 40 mL, supplementing with 1 M $MgCl_2$ (final concentration 1 mM), and incubating on ice for 3 min. Finally, the suspension was centrifuged at 5000× *g* for 15 min at 4 °C, and the supernatant was carefully collected.

α-syn was extracted using the osmotic shock method adapted from the study by Al-Azzawi et al. [15]. First, the biomass after overnight induction was centrifuged at 5000× *g* for 15 min at 4 °C. The cell pellet was then resuspended in 1X PBS solution and centrifuged again using the same parameters. The cell pellet was subsequently resuspended in Periplasmic Extraction Buffer A (30 mM Tris-HCl (pH 7.2); 40% (*w*/*v*) Sucrose; 2 mM EDTA) (5 mL of buffer per 50 mL of centrifuged bacterial culture). The suspension was incubated for 10 min at room temperature, then centrifuged at 9000× *g* for 20 min at 20 °C. The cells were then subjected to osmotic shock by rapidly resuspending the pellet in cold distilled water (5 mL of distilled water per 50 mL of centrifuged bacterial culture), followed by the addition of 1 M $MgCl_2$ (final concentration 1 mM) and incubation on ice for 3 min. The suspension was centrifuged at 9000× *g* for 30 min at 4 °C. The supernatant was carefully collected, filtered through a 0.22 µm membrane, and dialyzed overnight at 4 °C using a Dialysis Membrane (3.5K MWCO) in 50 mM Tris-HCl buffer, pH 8.3.

2.4. Purification of Nanobodies and α-syn Using the ÄKTA Start™ FPLC System

The crude periplasmic nanobody extract was purified by immobilized metal affinity chromatography (IMAC) using a HisTrap™ FF crude column (column volume 1 mL). The mobile phase included IMAC Binding Buffer (20 mM $Na^+PO_4^{3-}$; 300 mM NaCl; 5 mM Imidazole; pH 7.4) and IMAC Elution Buffer (20 mM $Na^+PO_4^{3-}$; 300 mM NaCl; 400 mM Imidazole; pH 7.4). The operating steps and corresponding parameters included the following: Column equilibration (8 CV, 1 mL/min); Sample loading (50 mL, 0.5 mL/min); Column washing (5 CV, 1 mL/min); Isocratic elution (8 CV, 1 mL/min), and Column re-equilibration (5 CV, 1 mL/min). Nanobody fractions displaying a clear peak

during the elution phase were collected, concentrated using an Amicon concentrator, analyzed by SDS-PAGE with the Laemmli buffer system, quantified for protein concentration via A280, and stored at −20 °C with 25% glycerol.

The periplasmic α-syn extract sample was purified by anion exchange chromatography (IEX) using a HiTrap™ Capto™ Q column (column volume 1 mL). The mobile phase included IEX Binding Buffer (50 mM Tris-HCl; pH 8.3) and IEX Elution Buffer (50 mM Tris-HCl; 750 mM NaCl; pH 8.3). The operating steps and corresponding parameters included: Column equilibration (8 CV, 1 mL/min); Sample loading (25 mL, 0.5 mL/min); Column washing (5 CV, 1 mL/min); Gradient elution (8 CV, Gradient 0–67–100%, 1 mL/min), and Column re-equilibration (5 CV, 1 mL/min). The sample was diluted 5-fold with IEX Binding Buffer before loading onto the column. The α-syn fraction exhibiting a clear peak during the elution phase also underwent analytical steps similar to those used for the nanobodies. Furthermore, the α-syn sample from *E. coli* W3110 Δ*ompC* induced with IPTG was selected as a representative to analyze the oligomeric states of α-syn via size-exclusion chromatography (SEC) using a HiPrep™ 16/60 Sephacryl™ S-100HR column. The mobile phase was 1X TBS; pH 7.4. Protein fractions with a clear peak during the elution phase were collected and analyzed by SDS-PAGE using the Laemmli buffer system.

2.5. Generation of Preformed Fibril α-syn (α-syn PFF) and Evaluation of α-syn Fibril-Forming Capacity via Thioflavin T Assay

Generation and validation via the ThT Assay of α-syn PFFs was adapted from the study by Joseph R. Patterson et al. [16]. First, the concentrated α-syn sample from W3110 Δ*ompC* (induced with IPTG) was centrifuged at 15,000× *g* for 10 min at 4 °C. The supernatant was transferred to a new, clean Eppendorf tube, and the α-syn concentration was recorded. The sample was diluted with dPBS (100 mM NaCl; 2.7 mM KCl; 10 mM Na_2HPO_4; 1.8 mM KH_2PO_4; pH 7–7.3) to a concentration of 5 mg/mL with a total volume of approximately 500 µL, and vortexed. The sample was filtered through a 0.22 µm membrane into a Protein LoBind tube. The tube was tightly sealed with parafilm and shaken on a thermoshaker at 37 °C, 1000 rpm for 7 days. The formation of oligomeric forms was monitored over the 7 days: every 24 h, 10 µL of the sample was collected to perform SDS-PAGE.

After 7 days of incubation, non-fibril α-syn (Day 1) or α-syn fibril (Day 7) samples were diluted 5 times in dPBS. Next, ThT Reaction Buffer (25 µM Thioflavin T; 100 mM Glycine; 1% (*v*/*v*) Triton X-100; pH 8.5) was added to each sample (1:1 ratio) and mixed gently. The mixture was transferred to a black 96-well plate (200 µL/well) and incubated for 1 h at room temperature. The results were read using an excitation wavelength of 450 nm and an emission wavelength of 510 nm. After confirming the presence of α-syn fibrils, sonication was performed to obtain the preformed fibril form: amplitude at 30%, cycle of 1 s pulse on, 1 s pulse off, pulse on time of 1 min.

2.6. Evaluation of Specific Binding Capacity to Alpha-Synuclein of Nanobodies via Indirect ELISA

First, non-fibril α-syn or α-syn PFF was diluted with Coating Buffer (0.2 M Sodium carbonate-bicarbonate; pH 9.4) (final concentration of approximately 11.4 µg/mL), then added to microplates (100 µL/well) and incubated overnight at 4 °C. The following day, the wells were washed 3 times with 1X PBST (200 µL/well) and Blocking Buffer (1X PBS; 5% (*w*/*v*) BSA) was added (200 µL/well). The wells were incubated for 1 h at 4 °C. The nanobody samples were initially diluted 10-fold with Dilution Buffer (1X PBS; 0.1% (*v*/*v*) Tween 20; 5% (*w*/*v*) BSA), followed by a 5-step serial dilution (DF = 2). The wells were then washed 3 times with 1X PBS (200 µL/well) and the corresponding nanobody dilution series was added (100 µL/well). Similarly, the wells were then washed 3 times with 1X PBST, Mouse 6x-His Tag Mab (diluted 4000-fold with Dilution Buffer) was added (100 µL/well),

washed 3 times again, and finally HRP-conjugated Goat anti-Mouse IgG (diluted 4000-fold with Dilution Buffer) was added (100 µL/well). The wells were incubated for 1 h at 4 °C, washed 3 times with 1X PBST, and Developing Buffer (51.5 mM Na_2HPO_4; 24.3 mM Citric acid; 0.006% (*v*/*v*) H_2O_2; 1 mg/mL TMB) was added. The wells were incubated for 30 min at room temperature and the colorimetric reaction was stopped by adding 2 M H_2SO_4 (100 µL/well). The reaction mixture in the wells was then measured spectrophotometrically at a wavelength of 450 nm (OD_{450}).

3. Results

3.1. Cloning of PFFNB2, MBP-PFFNB2, and α-syn

PFFNB2 was cloned into pBXNPH3 and pBXNPHM3, while α-syn was cloned into pTrcECT. The recombinant vectors, including pBXNPH3_PFFNB2 (P98), pBXNPHM3_PFFNB2 (P99), and pTrcECT_α-syn (ApTrc) (Figure 1), were then transformed into the *E. coli* DH5α strain for cloning. Colony PCR was performed using the pBAD Forward and pBAD Reverse primer pair to select colonies carrying P99 or P98. Similarly, colony PCR was performed using the PtrcPro-F and rrnB-T1-term-Rev primer pair to select colonies carrying ApTrc. Electrophoresis results demonstrated successful recombination of the insert into the vector pair, with PCR products displaying the expected sizes and the recombinant vectors extracted from these colonies also showing expected sizes. All detailed cloning results can be found in the Supplementary Materials (Figures S1 and S2).

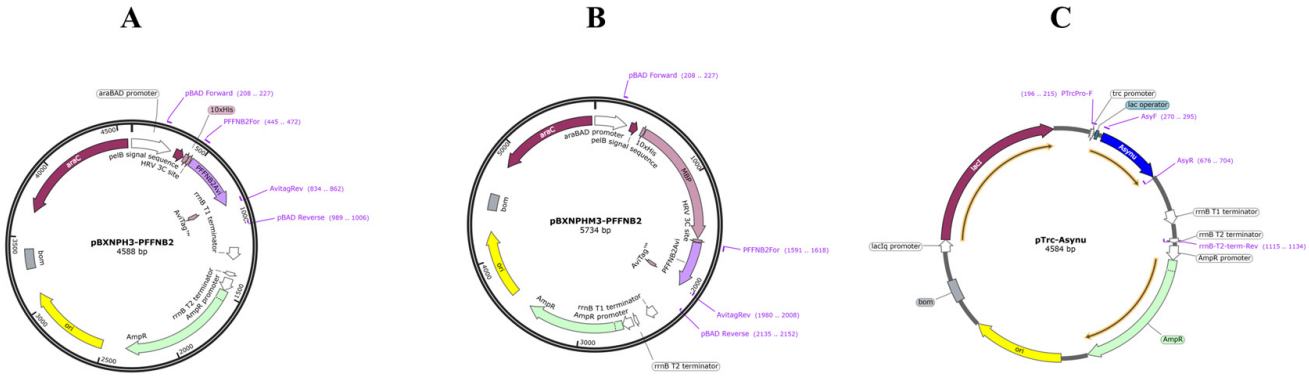

Figure 1. Recombinant vectors' map. (**A**) Vector map of pBXNPH3_PFFNB2 indicating the construct of pelB-10xHis-PFFNB2-Avitag. (**B**) Vector map of pBXNPHM3_PFFNB2 indicating the construct of pelB-10xHis-MBP-PFFNB2-Avitag. (**C**) Vector map of pTrcECT_ α-syn indicating the construct of tag-free α-syn. Created by SnapGene Software version 8.2.3 (ID 3281239).

3.2. Purification of Nanobodies and α-syn Using the ÄKTA start™ FPLC System

The chromatogram results from the purification of the nanobodies, including P98, P99 from *E. coli* W3110 (WP98, WP99) and P98, P99 from *E. coli* W3110 Δ*ompC* (EP98, EP99), using the IMAC method are presented in Figure 2. Overall, the nanobodies were successfully eluted at high imidazole concentrations (the system running 100% Elution Buffer, indicated by the Gradient Concentration line) with corresponding nanobody peaks at elution (retention) volumes (V_R) including WP98 (72.65 mL), EP98 (64.97 mL), WP99 (64.78 mL), and EP99 (64.66 mL).

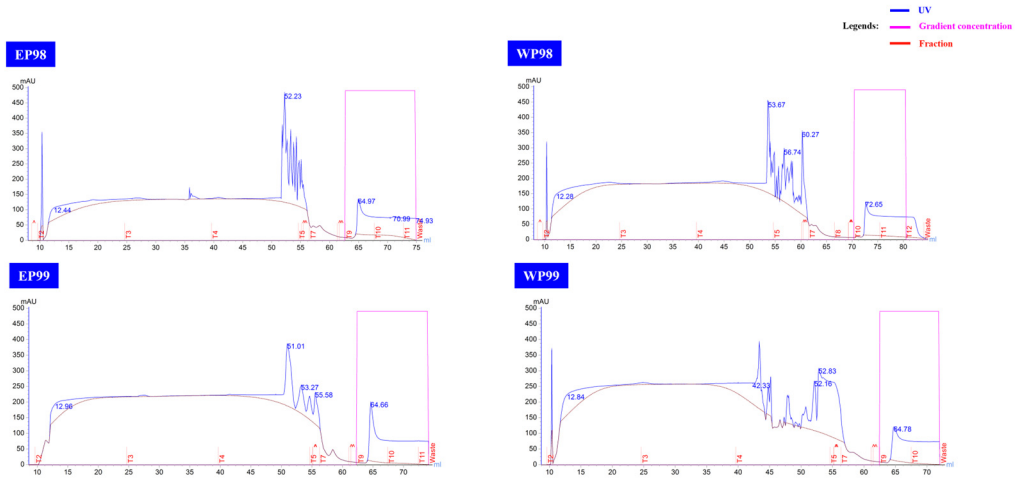

Figure 2. IMAC chromatogram results of nanobodies. Including: P98, P99 from *E. coli* W3110 (WP98, WP99) and P98, P99 from *E. coli* W3110 Δ*ompC* (EP98, EP99). The caret symbols (∧) along the baseline and fraction lines indicate the specific collection points of the eluted fractions recorded by the FPLC system. The chromatogram results from the purification of α-syn from *E. coli* W3110 (WA), and *E. coli* W3110 Δ*ompC* (EA), induced by IPTG or lactose (LAC), using the IEX method are presented in Figure 3. The peaks at a V_R between 42–48 mL indicate that α-syn was eluted at 67% Elution Buffer, corresponding to an NaCl concentration of 500 mM, as well as to Al-Azzawi et al.'s previous work [12].

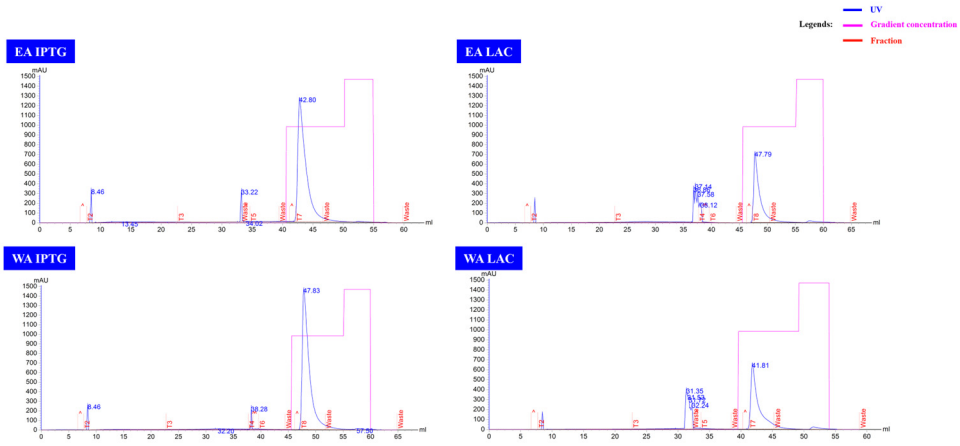

Figure 3. IEX chromatogram results of α-synuclein. Including α-syn from E. coli W3110 (WA), and E. coli W3110 Δ*ompC* (EA), induced by IPTG or lactose (LAC). The caret symbols (∧) along the baseline and fraction lines indicate the specific collection points of the eluted fractions recorded by the FPLC system.

3.3. SDS-PAGE of PFFNB2, MBP-PFFNB2, and α-syn Purified from E. coli W3110 and W3110 ΔompC

Both *E. coli* W3110 and W3110 Δ*ompC* strains successfully expressed PFFNB2 with similar sizes ranging from 13 to 15 kDa (Figure 4A). On the other hand, MBP-PFFNB2 was expressed with a low degree of oligomerization; however, the Δ*ompC* mutant yielded a product size lower than the expected size (approximately 58 kDa) (Figure 4B). Under both reducing and non-reducing conditions using β-mercaptoethanol, the MBP-PFFNB2s exhibited similar sizes, proving that the absolute disulfide bond-free structure of the MBP-PFFNB2s was preserved.

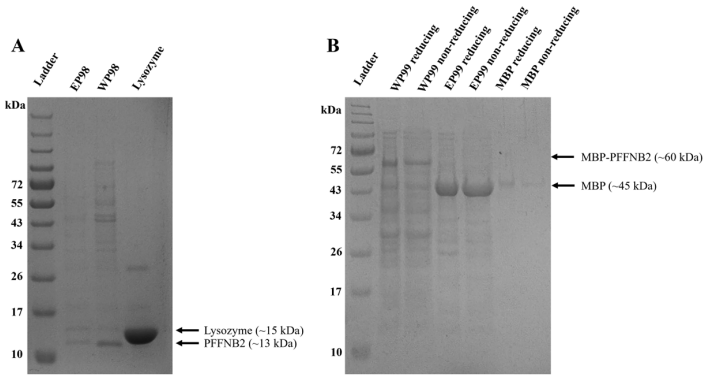

Figure 4. SDS-PAGE results for the nanobodies. (**A**) Tag-free PFFNB2 from both strains show a prominent band at around 13 kDa (Lysozyme, 15 kDa, at a concentration of 0.5 µg/mL for comparison). (**B**) MBP-PFFNB2 with clear different sizes between two strains under both reducing (β-mercaptoethanol employed) and non-reducing conditions (MBP, 45 kDa, at a concentration of 0.5 mg/mL for comparison).

Regarding α-syn, both strains successfully expressed α-syn with similar monomeric size (~20 kDa) (Figure 5A). This size shift can be explained by the negatively charged C-terminal region of α-syn causing SDS resistance on the SDS-PAGE gel [17]. About the conformation of the α-syn product, after 10 h of IPTG induction, both *E. coli* W3110 and the Δ*ompC* mutant yielded products presenting simultaneously both the monomeric form and oligomeric forms including dimers (~30 kDa), trimers (~40 kDa), and tetramers (~60 kDa). When analyzed by SEC, the results showed that the majority of α-syn in the sample existed as dimers with a high UV signal of nearly 60 mAu in fraction T7 (Figure 5B). In contrast, after 10 h of lactose induction, both expression strains yielded products with almost no presence of high-order oligomeric forms, leaving only the monomeric and dimeric forms.

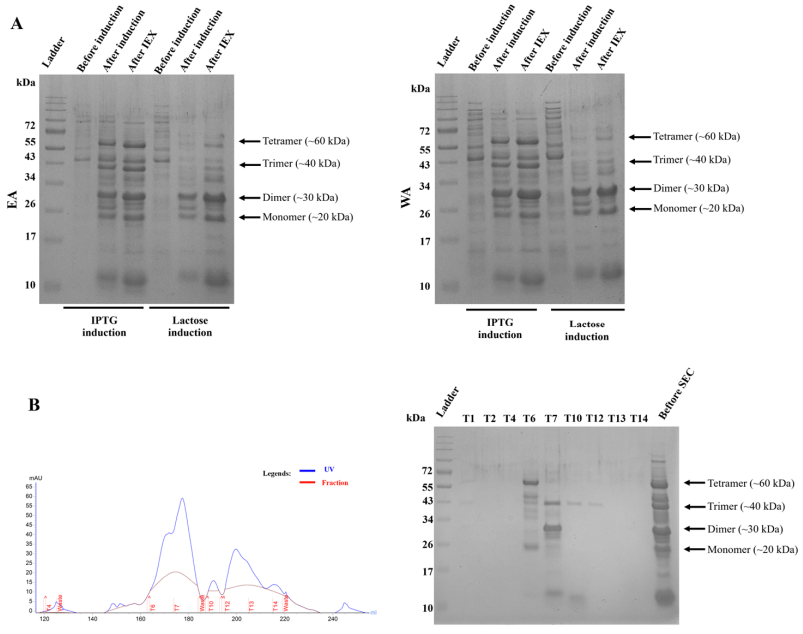

Figure 5. SDS-PAGE results for α-syn. (**A**) Different α-syn's conformations visible for both strains with both inducers. Notably, under Lactose's induction, there is a reduction in oligomeric forms (Trimer and Tetramer of α-syn). (**B**) SEC chromatogram and corresponding SDS-PAGE gel of different fractions, including the previously purified and concentrated sample (before SEC). The caret symbols (∧) along the baseline and fraction lines indicate the specific collection points of the eluted fractions recorded by the FPLC system.

3.4. Expression Yield of Nanobodies and α-syn in the Two E. coli Strains

The nanobody expression yield showed clear differences (Figure 6A): MBP-PFFNB2 was expressed with higher yield than the non-MBP fused form in both *E. coli* strains, with the *E. coli* W3110 strain providing better expression yield than the Δ*ompC* mutant. Conversely, the Δ*ompC* mutant yielded a higher expression yield for the non-MBP fused form than the wild-type strain. Compared to the nanobodies, the α-syn expression yield demonstrated a pronounced difference, as the *E. coli* W3110 Δ*ompC* strain yielded higher yield results over the non-mutated strain (Figure 6B) in both cases of induction with IPTG or lactose. All A_{280} values retrieved from Nanodrop are given in Supplementary Materials (Figure S3).

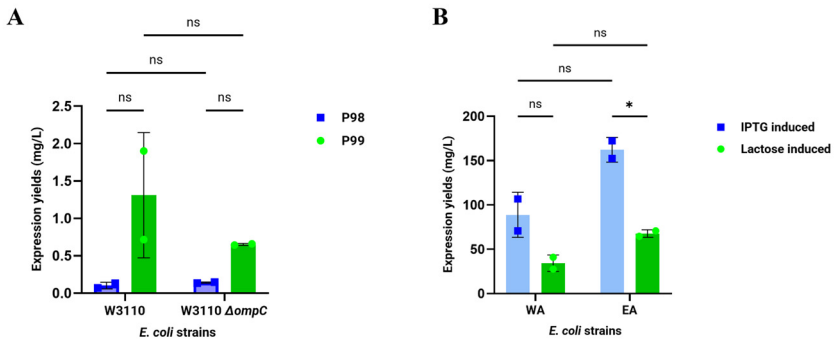

Figure 6. Comparison of expression yield between the 2 nanobody forms and α-syn in the *E. coli* strains. Expression yields (mg protein/Liter of culture) of nanobodies (**A**) and α-syn under different inducers' influence (**B**). Data are presented as mean ± SD ($n = 2$ independent biological replicates). Statistical significance was determined using Two-Way ANOVA, where **ns** indicates no significant difference ($p > 0.1$) and ***** indicates statistical significance ($p = 0.1$).

3.5. Formation of α-syn PFF Demonstrated via ThT Assay and SDS-PAGE

The formation of the amyloid fibril form of α-syn was monitored over 7 days on an SDS-PAGE gel (Figure 7A). The results revealed that α-syn underwent a conformational transition from a mixture of monomers and oligomers to predominantly oligomeric forms after 7 days. Concurrently, the ThT Assay results showed that the fluorescence signal of the α-syn sample after 7 days was significantly higher compared to the initial day and the dPBS blank (Figure 7B).

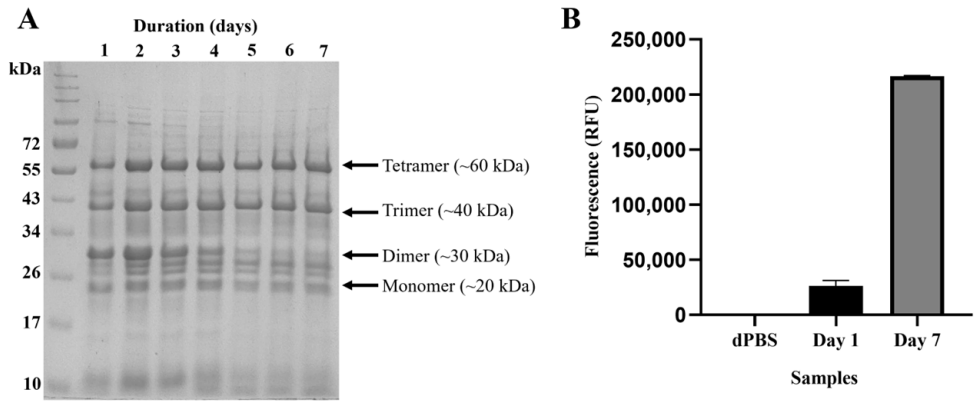

Figure 7. Conformational transition process of α-syn and reaction results with Thioflavin T confirming the presence of α-syn fibrils. (**A**) SDS-PAGE gel demonstrating a conformational shift of α-syn from mixtures of monomer and oligomers to mostly oligomers throughout a 7-day period. (**B**) Thioflavin T fluorescence signal amplified by the presence of α-syn fibrils after 7-day incubation.

3.6. Evaluation of Specific Binding Capacity α-syn of Nanobodies via ELISA

A four-parameter logistic curve model was applied to determine apparent EC_{50} values in order to evaluate and compare the activity of the four nanobodies WP98, EP98, WP99, and EP99 in binding reactions with non-fibril α-syn and α-syn PFF. All experiments were performed in $n = 2$ independent biological replicates. For non-fibril α-syn, EP99 exhibited the strongest apparent binding potency with an EC_{50} value of 0.4212 nM, followed by EP98 with an EC_{50} of 0.5090 nM (Figure 8A). In contrast, WP98 and WP99 produced virtually no binding signals to the antigen. More notably, for α-syn PFF, EP99 was the sole nanobody generating data highly consistent with the antigen–antibody binding kinetics model (Figure 8B). The EC_{50} value of EP99 was 0.3445 nM. Conversely, the EC_{50} values for EP98, WP98, and WP99 lacked statistical significance under the investigated conditions.

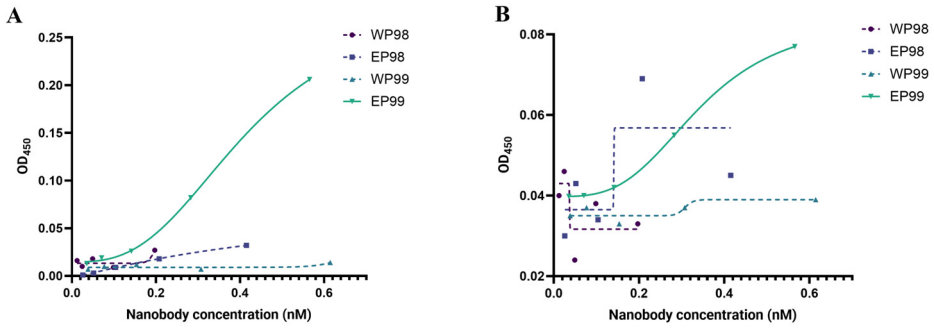

Figure 8. Sigmoidal graphs representing the apparent binding potency of the nanobodies to different α-syn forms by concentration. (**A**) Apparent binding potency of nanobodies towards non-fibril α-syn. (**B**) Apparent binding potency of nanobodies towards α-syn PFF.

4. Discussion

Typically, studies leverage the chaperone system within the periplasmic space of *E. coli* to facilitate oxidation for disulfide bond formation, thereby assisting the protein in folding correctly into its native structure. However, PFFNB2 does not contain any disulfide bonds, could only be expressed as an MBP fusion, and had to be accompanied by GroES/GroEL chaperones. Nonetheless, co-expression with chaperones carries side effects such as unintentionally activating protein degradation pathways to resolve inclusion bodies, placing a burden on the host cell's metabolic machinery that reduces expression yield, or even forming pseudo-inclusion bodies that, while soluble, lack biological activity [18]. Meanwhile, when directing PFFNB2 to the periplasm, alongside the canonical DsbA and DsbB system, the periplasm is also equipped with disulfide bond-independent chaperones such as SurA, Skp, FkpA, and DegP [19]. Tag-free PFFNB2 expressed in the periplasmic space was demonstrated to possess activity against non-fibril α-syn, proving that the potential of expressing nanobodies in the periplasmic space of *E. coli* can be applied even to nanobodies with special structures like PFFNB2. However, the activity of PFFNB2 was inferior to that of the MBP-PFFNB2 fusion towards non-fibril α-syn ($EC_{50}{}^{EP99} = 0.4212$ nM, $EC_{50}{}^{EP98} = 0.5090$ nM). It is hypothesized that although PFFNB2 folded sufficiently to remain soluble in solution, upon approaching α-syn, PFFNB2 might have been unable to self-maintain its structure to access the α-syn epitope. Thus, it is possible that PFFNB2 still requires MBP, which intrinsically also functions as a chaperone, to help stabilize its structure and function. This phenomenon was previously observed in the study by Horacio Bach et al. [20]. Another notable point is that while studies typically indicate that MBP causes partial steric hindrance making it difficult for the nanobody to comprehensively access the antigen [21], in the case of PFFNB2, MBP plays a more crucial role in preserving the nanobody's activity rather than obstructing it from binding to α-syn.

The most prominent finding is that only the nanobodies expressed and purified from the *E. coli* W3110 Δ*ompC* strain yielded genuine apparent binding potency for the target α-syn (statistically significant EC_{50}). Among them, although the product size of EP99 was lower than expected, only this nanobody exhibited genuine high apparent binding potency for α-syn PFF, which is the primary target of PFFNB2. Therefore, it is plausible that within the periplasmic space of the Δ*ompC* mutant, MBP-PFFNB2 tightly compacted its structure, causing its size shown on the electrophoresis gel to be smaller than theoretically expected and compared to WP99. The hypothesis proposed is that the mutation deleting this porin impacted the outer membrane structure, causing an accumulation of defective membrane proteins or an osmotic pressure imbalance in the periplasm [22]. This robustly triggers cell envelope stress response pathways, including an upregulation in the expression levels of chaperones such as Skp, SurA, FkpA, and the DsbA/DsbB disulfide bond-catalyzing system. In EP99, although the product size of EP99 was lower than expected, we hypothesize as a working hypothesis that MBP-PFFNB2 might have adopted a more compact conformation within the periplasm of the Δ*ompC* mutant, subsequently migrating faster on the electrophoresis gel, similar to the case of tag-free PFFNB2. And as it was enhanced in folding and structurally defined by the foldase system of the EP99 strain, including MBP itself, the apparent binding potency of PFFNB2 for alpha-synuclein may increase compared to WP99 and EP98. However, while MBP is essential to maintain nanobody stability and activity during recombinant bacterial expression, its large molecular size might pose a distinct challenge regarding blood–brain barrier penetration, which must be addressed via tag cleavage or alternative delivery strategies in future translational developments. Furthermore, the integration of the Avitag sequence at the C-terminus of the engineered nanobodies provides a versatile platform for site-specific biotinylation in future studies. This will enable high-oriented immobilization of PFFNB2 onto streptavidin-coated surfaces for advanced biosensing or diagnostic evaluations of α-synuclein aggregates.

Regarding α-syn, preliminary results showed that α-syn predominantly existed in the dimeric form within the sample. A working hypothesis is that under the oxidative conditions of the periplasmic space, tyrosine residues in the α-syn structure easily covalently pair to form stable dityrosine crosslinks (ortho-ortho bonds), as observed by Al-Hilaly et al. [23]. These homodimer molecules are highly stable, even capable of resisting SDS. In addition, it can be seen that the use of lactose as an inducer helped α-syn form fewer high-order oligomeric species when expressed in both *E. coli* strains, forms that have been proven to be toxic to the host *E. coli* cells themselves, not just in mammals [24]. Concerning the α-syn expression yield, there was a notable difference where the *E. coli* W3110 Δ*ompC* strain provided higher yield results compared to the non-mutated strain. This phenomenon can be explained by the increased inducer uptake capacity of the Δ*ompC* mutant, supported by findings from Hosni Sassi et al. [11]. Consequently, IPTG or lactose could easily diffuse directly into the intracellular space without relying entirely on active transport channels, allowing the cells to receive higher inducer concentrations, thereby activating the protein expression system more rapidly and efficiently than the wild-type *E. coli* W3110 strain.

5. Conclusions

The study successfully demonstrated the recombinant periplasmic expression and subsequent purification of PFFNB2 and MBP-PFFNB2, a novel finding compared to the original study by Yemima et al. where PFFNB2 had only been successfully expressed as an MBP fusion in the cytoplasm of *E. coli*, alongside chaperone assistance. Although the proteins were expressed at the correct MWs according to SDS-PAGE, MBP-PFFNB2 exhibited better activity on the target α-syn than PFFNB2 alone. Furthermore, when comparing the expression strains, despite yielding a lower expression yield, *E. coli* W3110 Δ*ompC* produced

a nanobody with higher activity compared to the non-mutated strain, especially since only MBP-PFFNB2 from the Δ*ompC* mutant possessed the capability to specifically bind to α-syn PFF, the primary target of the nanobody. However, further orthogonal biophysical and process-scale optimizations are required for broader translational applications. The study also concurrently expressed and purified tag-free α-syn on the pTrc vector system, utilizing two different inducers across both *E. coli* W3110 and *E. coli* W3110 Δ*ompC* strains. In this context, *E. coli* W3110 Δ*ompC* delivered higher expression yield over the non-mutated strain, and the use of lactose at a 2% concentration facilitated the partial elimination of high molecular weight oligomeric forms of α-syn.

Supplementary Materials: The following supporting information can be downloaded at: https://www.mdpi.com/article/10.3390/cimb48111104/s1.

Author Contributions: Methodology, Investigation, Writing—original draft, H.N.-T.; Data curation, Formal analysis, Supervision, Validation, A.N.-T.; Conceptualization, Funding acquisition, Writing—review and editing, T.N.-M. All authors have read and agreed to the published version of the manuscript.

Funding: This work has received support from the Korea International Cooperation Agency (KOICA) [Project No. 2021-00020-3]. The funding sponsor had no involvement in the study design, collection, analysis and interpretation of data, writing of the report, and decision to submit the article for publication.

Institutional Review Board Statement: Not applicable.

Informed Consent Statement: Not applicable.

Data Availability Statement: The original contributions presented in this study are included in the article/Supplementary Material. Further inquiries can be directed to the corresponding author.

Conflicts of Interest: The authors declare no conflicts of interest.

References

1. Teymourian, H.; Tehrani, F.; Longardner, K.; Mahato, K.; Podhajny, T.; Moon, J.-M.; Kotagiri, Y.G.; Sempionatto, J.R.; Litvan, I.; Wang, J. Closing the loop for patients with Parkinson disease: Where are we? *Nat. Rev. Neurol.* **2022**, *18*, 497–507. [CrossRef] [PubMed]
2. Morris, H.R.; Spillantini, M.G.; Sue, C.M.; Williams-Gray, C.H. The pathogenesis of Parkinson's disease. *Lancet* **2024**, *403*, 293–304. [CrossRef] [PubMed]
3. Wankhede, N.L.; Kale, M.B.; Upaganlawar, A.B.; Taksande, B.G.; Umekar, M.J.; Behl, T.; Abdellatif, A.A.; Bhaskaran, P.M.; Dachani, S.R.; Sehgal, A.; et al. Pharmacotherapy, Involvement of molecular chaperone in protein-misfolding brain diseases. *Biomed. Pharmacother.* **2022**, *147*, 112647. [CrossRef] [PubMed]
4. Hmila, I.; Vaikath, N.N.; Majbour, N.K.; Erskine, D.; Sudhakaran, I.P.; Gupta, V.; Ghanem, S.S.; Islam, Z.; Emara, M.M.; Abdesselem, H.B.; et al. Novel engineered nanobodies specific for N-terminal region of alpha-synuclein recognize Lewy-body pathology and inhibit in-vitro seeded aggregation and toxicity. *FEBS J.* **2022**, *289*, 4657–4673. [CrossRef] [PubMed]
5. De Genst, E.J.; Guilliams, T.; Wellens, J.; O'DAy, E.M.; Waudby, C.A.; Meehan, S.; Dumoulin, M.; Hsu, S.-T.D.; Cremades, N.; Verschueren, K.H.; et al. Structure and Properties of a Complex of α-Synuclein and a Single-Domain Camelid Antibody. *J. Mol. Biol.* **2010**, *402*, 326–343. [CrossRef] [PubMed]
6. Guilliams, T.; El-Turk, F.; Buell, A.K.; O'Day, E.M.; Aprile, F.A.; Esbjörner, E.K.; Vendruscolo, M.; Cremades, N.; Pardon, E.; Wyns, L.; et al. Nanobodies Raised against Monomeric α-Synuclein Distinguish between Fibrils at Different Maturation Stages. *J. Mol. Biol.* **2013**, *425*, 2397–2411. [CrossRef] [PubMed]
7. Butler, D.C.; Joshi, S.N.; Genst, E.D.; Baghel, A.S.; Dobson, C.M.; Messer, A. Bifunctional Anti-Non-Amyloid Component α-Synuclein Nanobodies Are Protective In Situ. *PLoS ONE* **2016**, *11*, e0165964. [CrossRef] [PubMed]
8. Butler, Y.R.; Liu, Y.; Kumbhar, R.; Zhao, P.; Gadhave, K.; Wang, N.; Li, Y.; Mao, X.; Wang, W. α-Synuclein fibril-specific nanobody reduces prion-like α-synuclein spreading in mice. *Nat. Commun.* **2022**, *13*, 4060. [CrossRef] [PubMed]
9. Sandomenico, A.; Sivaccumar, J.P.; Ruvo, M. Evolution of Escherichia coli expression system in producing antibody recombinant fragments. *Int. J. Mol. Sci.* **2020**, *21*, 6324. [CrossRef] [PubMed]

10. Lück, R.; Zimmermann, C.; Spadiut, O.; Kopp, J. Intensified upstream processing by a phosphate-regulated, auto-inducible expression system in *E. coli* W3110 for recombinant Fab production. *BMC Microbiol.* **2026**, *26*, 375. [CrossRef] [PubMed]
11. Sassi, H.; Nguyen, T.M.; Telek, S.; Gosset, G.; Grünberger, A.; Delvigne, F. Segregostat: A novel concept to control phenotypic diversification dynamics on the example of Gram-negative bacteria. *Microb. Biotechnol.* **2019**, *12*, 1064–1075. [CrossRef] [PubMed]
12. Zimmermann, I.; Egloff, P.; Hutter, C.A.; Arnold, F.M.; Stohler, P.; Bocquet, N.; Hug, M.N.; Huber, S.; Siegrist, M.; Hetemann, L.; et al. Synthetic single domain antibodies for the conformational trapping of membrane proteins. *eLife* **2018**, *7*, e34317. [CrossRef] [PubMed]
13. Ning, Y.; Wu, X.; Zhang, C.; Xu, Q.; Chen, N.; Xie, X. Pathway construction and metabolic engineering for fermentative production of ectoine in Escherichia coli. *Metab. Eng.* **2016**, *36*, 10–18. [CrossRef] [PubMed]
14. Zimmermann, I.; Egloff, P.; Hutter, C.A.J.; Kuhn, B.T.; Bräuer, P.; Newstead, S.; Dawson, R.J.P.; Geertsma, E.R.; Seeger, M.A. Generation of synthetic nanobodies against delicate proteins. *Nat. Protoc.* **2020**, *15*, 1707–1741. [CrossRef] [PubMed]
15. Al-Azzawi, Z.A.M.; Silver, N.R.G.; Mehra, S.; Niu, S.; Situ, C.; Luo, W.; Shlaifer, I.; Ingelsson, M.; Hyman, B.T.; Trempe, J.F.; et al. α-Synuclein purification significantly impacts seed amplification assay performance and consistency. *Acta Neuropathol. Commun.* **2025**, *13*, 225. [CrossRef] [PubMed]
16. Patterson, J.R.; Polinski, N.K.; Duffy, M.F.; Kemp, C.J.; Luk, K.C.; Volpicelli-Daley, L.A.; Kanaan, N.M.; Sortwell, C.E. Generation of Alpha-Synuclein Preformed Fibrils from Monomers and Use In Vivo. *J. Vis. Exp.* **2019**, *148*, e59758. [CrossRef] [PubMed]
17. Coelho-Cerqueira, E.; Carmo-Gonçalves, P.; Pinheiro, A.S.; Cortines, J.; Follmer, C. α-Synuclein as an intrinsically disordered monomer–fact or artefact? *FEBS J.* **2013**, *280*, 4915–4927. [CrossRef] [PubMed]
18. Martínez-Alonso, M.; García-Fruitós, E.; Ferrer-Miralles, N.; Rinas, U. Villaverde, Side effects of chaperone gene co-expression in recombinant protein production. *Microb. Cell Fact.* **2010**, *9*, 64. [CrossRef] [PubMed]
19. Stull, F.; Betton, J.-M.; Bardwell, J.C. Periplasmic chaperones and prolyl isomerases. *EcoSal Plus* **2018**, *8*, 10–1128. [CrossRef] [PubMed]
20. Bach, H.; Mazor, Y.; Shaky, S.; Shoham-Lev, A.; Berdichevsky, Y.; Gutnick, D.L.; Benhar, I.J. Escherichia coli maltose-binding protein as a molecular chaperone for recombinant intracellular cytoplasmic single-chain antibodies. *J. Mol. Biol.* **2001**, *312*, 79–93. [CrossRef] [PubMed]
21. Salema, V.; Fernández, L.Á. High yield purification of nanobodies from the periplasm of *E. coli* as fusions with the maltose binding protein. *Protein Expr. Purif.* **2013**, *91*, 42–48. [CrossRef] [PubMed]
22. Hasenbein, S.; Merdanovic, M.; Ehrmann, M.J.G. Determinants of regulated proteolysis in signal transduction. *Genes Dev.* **2007**, *21*, 6–10. [CrossRef] [PubMed]
23. Al-Hilaly, Y.K.; Biasetti, L.; Blakeman, B.J.; Pollack, S.J.; Zibaee, S.; Abdul-Sada, A.; Thorpe, J.R.; Xue, W.F.; Serpell, L.C. The involvement of dityrosine crosslinking in α-synuclein assembly and deposition in Lewy Bodies in Parkinson's disease. *Sci. Rep.* **2016**, *6*, 39171. [CrossRef] [PubMed]
24. Kamboj, S.; Harms, C.; Kumar, L.; Creamer, D.; West, C.; Klein-Seetharaman, J.; Sarkar, S.K. A method of purifying alpha-synuclein in *E. coli* without chromatography. *Heliyon* **2021**, *7*, e05874. [CrossRef] [PubMed]

Disclaimer/Publisher's Note: The statements, opinions and data contained in all publications are solely those of the individual author(s) and contributor(s) and not of MDPI and/or the editor(s). MDPI and/or the editor(s) disclaim responsibility for any injury to people or property resulting from any ideas, methods, instructions or products referred to in the content.